A Novel Alternating Cell Directions Implicit Method for the Solution of Incompressible Navier Stokes Equations on Unstructured Grids

O. Bas[1], A. R. Cete[2†], S. Mengi[2], I. H. Tuncer[3] and U. Kaynak[4]

[1] Turkish Aerospace Industries Inc, Ankara, Turkey,
[2] Gaziantep University, Gaziantep, Turkey
[3] Middle East Technical University, Ankara, Turkey
[4] TOBB University of Economics and Technology, Ankara, Turkey

†Corresponding Author Email: arcete@gantep.edu.tr

ABSTRACT

In this paper, A Novel Alternating Cell Direction Implicit Method (ACDI) is researched which allows implementation of fast line implicit methods on quadrilateral unstructured meshes. In ACDI method, designated alternating cell directions are taken along a series of contiguous cells within the unstructured grid domain and used as implicit lines similar to Line Gauss Seidel Method (LGS). ACDI method applied earlier for the solution of potential flows is extended for the solution of the incompressible Navier-Stokes equations on unstructured grids. The system of equations is solved by using the Symmetric Line Gauss-Seidel (SGS) method along the alternating cell directions. Laminar flow fields over a single element NACA-0008 airfoil are computed by using structured and unstructured quadrilateral grids, and inviscid Euler flow solutions are given for the NACA-23012b multielement airfoil. The predictive capability of the method is validated against the data taken from the experimental or the other numerical studies and the efficiency of the ACDI method is compared with the implicit Point Gauss Seidel (PGS) method. In the selected validation cases, the results show that a reduction in total computation between 18% and 23% is achieved by the ACDI method over the PGS. In general, the results show that the ACDI method is a fast, efficient, robust and versatile method that can handle complicated unstructured grid cases with equal ease as with the structured grids.

Keywords: Alternating cell directions implicit method; ACDI; U-MUSCL; Artificial compressibility; Incompressible N-S solver.

NOMENCLATURE

A	area	$\vec{r}$	position vector
$\overline{A}$	flux jacobian	Re	Reynolds number
$\vec{F_c}$	convective flux	S	length
$\vec{F_v}$	viscous flux	Q	flow variables
$\vec{I}$	unit vector	u,v	velocity component
P	pressure	β	artificial compressibility parameter
$\vec{R}$	residual vector	Δt	time step

1. INTRODUCTION

General trends such as reducing grid generation time and increasing the robustness, accuracy and time efficiency of the solvers are still valid in the computational fluid dynamics community. There are ongoing research, especially on unstructured grid generators and solvers, high order schemes and fast implicit methods.

The most common schemes used for temporal discretisation of the governing equations can be classified into two main groups which are explicit and implicit methods. In general, it is known that explicit methods are easy to implement and solution steps are not computationally expensive, whereas

implicit methods have better convergence characteristics and are less dependent on computational grids compared with the explicit methods. Increasing reputation of implicit schemes for steady-state problem solutions is caused from their two remarkable properties which are the robustness and the time efficiency.

Full implicit Sato *et al.* (2003); Chan and Anastasiou (1999) and point implicit Sheng and Whitfield (1999) methods are the most commonly used techniques for solvers on unstructured grids. However, well established and widely used line implicit methods such as Line Gauss Seidel Rogers and Kwak (1990) and Alternating Directions Implicit (ADI) Duc (1999); Kaliakatsos *et al.* (1996) methods are mostly employed on structured grid solvers. Comparison of these implicit solution methods are given in the references Yuan (2002); Rogers (1995) and Anderson *et al.* (1996).

In general, the line implicit methods have an advantage over the point implicit methods in terms of time efficiency. Besides, requirement of less computer resources is another remarkable benefit of them when they compared with the full implicit schemes. However, the line implicit methods are not applicable on unstructured grids in their conventional forms. Recently, a novel method was proposed by Çete and Kaynak (2006); Çete (2004) that implements a line implicit method on unstructured grids, which is called Alternating Cell Directions Implicit, ACDI. In this new method, a series or a chain of contiguous cells are used to form implicit solution bands in such a way that the entire flow field is covered by passing over each cell twice. The solution on each solution band is performed similar to the Gauss-Seidel method. The method is shown to be fast and accurate similar to the ADI. This method was first applied to potential flows and showed equal levels of efficiency on both the structured and unstructured grids.

On the other hand, in recent years, developing an incompressible Navier-Stokes solvers which are robust and efficient has gain importance for design and analysis purposes of unmanned air vehicles, wind turbines, bio-fluids and etc. Although the incompressible N-S equations constitute a subset of the compressible N-S equations, they are treated separately and in general are more difficult to solve. Numerous methodologies and algorithms can be found in the literature for the solution of incompressible flow equations. These solution methods fall under three main categories: vorticity-stream function method, pressure based methods and density based methods. Among these various methods, the artificial compressibility Chorin (1967) formulation which is included in the density based methods category is chosen in the present work because of its wide usage and similarity with the compressible flow equations. This similarity allows implementation of most of the methods developed and successfully used in the compressible flow solvers.

In the present paper, the ACDI method is extended to the solution of incompressible Navier-Stokes

equations on unstructured quadrilateral grids. The efficiency and stability of the ACDI method are studied in detail.

2. ALTERNATING CELL DIRECTIONS IMPLICIT METHOD

Utilization of sequential cell directions formed the main structure of the idea behind the ACDI method. These directions are used for creating solution bands which are essential in all line implicit methods. It is possible to define directions passing through the mutual edges of quadrilateral cells as shown in Fig. 1. Solution bands are generated by combining the lines passing through these mutual edges. These bands pass twice from each quadrilateral element. There are two valid directions for each solution bands and these directions depends on the choice of the starting edge. However, both direction can be used for the solution process without making any difference of the results. The main difference between these two direction is taking one direction as implicit and the other one as explicit which yields a three diagonal matrix system.
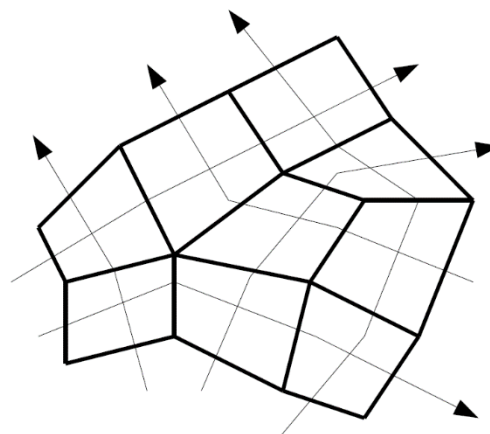

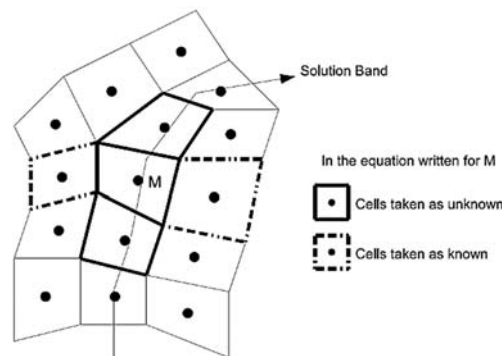**Fig. 1. A Sample Grid Portion with Solution Bands.**

Fig. 2. General Cell Structure.

For single blocked structured grids, the sequential cell directions coincide with the curvilinear coordinates, but for unstructured grids, it becomes possible to obtain a direction concept by using this method. Once the solution bands are generated, it

becomes possible to apply line implicit methods with some modifications. Fig. 2 shows a solution band on a sample grid. As seen in Fig. 2, the flux computation on cell "M" are coupled to the cells L and N, which eventually leads to a tridiagonal load matrix to be solved.

3. FLOW SOLVER

The governing equations used in this work are two dimensional incompressible Navier-Stokes equations with artificial compressibility modification. Laminar and constant viscosity flows without body forces are considered. The resulting set of equations for an arbitrary grid is given in integral form as

$$\frac{\partial}{\partial t}\int_A Q dA + \oint_S \left(\vec{F}_c - \vec{F}_v\right).\hat{n}dS = 0 \tag{1}$$

where Q is the vector of independent variables, including pressure and velocity components, F_c is the convective flux and F_v represents the viscous flux vectors.

$$Q = \begin{pmatrix} P \\ u \\ v \end{pmatrix} \quad , \vec{F}_c = \begin{pmatrix} \beta\left(u.\vec{i} + v.\vec{j}\right) \\ \left(u^2 + p\right).\vec{i} + \left(uv\right).\vec{j} \\ \left(uv\right).\vec{i} + \left(v^2 + p\right).\vec{j} \end{pmatrix}$$

$$\vec{F}_v = \frac{1}{Re}\begin{vmatrix} 0 \\ \frac{\partial u}{\partial x}.\vec{i} + \frac{\partial u}{\partial y}.\vec{j} \\ \frac{\partial v}{\partial x}.\vec{i} + \frac{\partial v}{\partial y}.\vec{j} \end{vmatrix}$$

In Eq. (1), β and Re represents the artificial compressibility coefficient and the Reynolds number respectively, and $\hat{n}$ is the outward-pointing unit normal of the corresponding control volume boundary.

3.1 Spatial Discretisation

A cell centered finite volume method is used in this study for the spatial discretisation of the governing equations over quadrilateral elements. Derivatives are evaluated using Green-Gauss theorem while piecewise constant, piecewise linear and U-MUSCL schemes are applied for the evaluation of the flow variables over the cell edges. The convective terms of artificial compressibility formulation have a hyperbolic character and upwinding technique is used to obtain stable solutions. On the other hand, viscous terms are elliptical nature and a central discretisation is employed.

It is well known that central discretisation causes series stability problems in convective terms and upwinding is the most widely used solution to this problem. When artificial compressibility formulation is considered, it is important to note that the convective fluxes do not have the homogeneity property. This property can be shown with the

necessity of the equality given below,

$$F = \frac{\partial F}{\partial Q}Q \tag{2}$$

Since the absence of homogeneity property, the flux vector splitting schemes can not be used in this formulation. The convective terms can be discretized by using Roe flux difference splitting scheme and central discretisation is employed for viscous fluxes. The general formula of the Roe approximate Riemann solver is given by

$$F_{i+\frac{1}{2}} = \frac{1}{2}.\left[F\left(Q_L\right) + F\left(Q_R\right) - \left|\bar{A}_{Roe}\right|.\left(Q_R - Q_L\right)\right] \tag{3}$$

where $\left|\bar{A}_{Roe}\right|$ term represents the Roe averaged flux Jacobian matrix. Roe averaging is a simple arithmetic averaging in the modified version of the Navier-Stokes equations for incompressible case. The flux Jacobian matrix can be defined as,

$$\bar{A} = \frac{\partial F}{\partial Q} = \begin{pmatrix} 0 & \beta\vec{i} & \beta\vec{j} \\ \vec{i} & \vec{V} + u\vec{i} & u\vec{j} \\ \vec{j} & v\vec{i} & \vec{V} + u\vec{j} \end{pmatrix}$$

$\lambda_1 = \vec{V}$, $\lambda_2 = \left(\vec{V} + c\right)$ and $\lambda_3 = \left(\vec{V} - c\right)$ are the eigen-values of the flux Jacobian matrix. "c" which is equal to $\sqrt{\vec{V}^2 + \beta}$ epresents the artificial speed of sound.

$\left|\bar{A}_{Roe}\right|$ term can be evaluated for each edge by using the following formula,

$$\left|\bar{A}\right| = T\left|\Lambda\right|T^{-1} \tag{4}$$

In the Eq. (4), T and T^{-1} represents the right eigen-vectors and the inverse of the right eigenvectors of the flux Jacobian, respectively. The all terms of the diagonal matrix $|\Lambda|$ are the absolute values of the eigenvalues. These matrices can be written as,

$$|\Lambda| = \begin{pmatrix} |\lambda_1| & 0 & 0 \\ 0 & |\lambda_2| & 0 \\ 0 & 0 & |\lambda_3| \end{pmatrix}$$

$$T = \begin{pmatrix} 0 & -c\left[\vec{V} - c\right] & c\left[\vec{V} + c\right] \\ -\vec{j} & \left(c\vec{i} - \phi\vec{j}\right) & -\left(c\vec{i} + \phi\vec{j}\right) \\ \vec{i} & \left(c\vec{j} + \phi\vec{i}\right) & -\left(c\vec{j} - \phi\vec{i}\right) \end{pmatrix}$$

$$T^{-1} = \begin{pmatrix} -\dfrac{\phi}{c^2} & \dfrac{\phi\vec{V}\vec{i} + c^2\vec{j}}{c^2} & -\dfrac{\phi\vec{V}\vec{j} - c^2\vec{i}}{c^2} \\ \dfrac{1}{2c^2} & \dfrac{\left(\vec{V} + c\right)\vec{i}}{2c^2} & \dfrac{\left(\vec{V} + c\right)\vec{j}}{2c^2} \\ \dfrac{1}{2c^2} & \dfrac{\left(\vec{V} - c\right)\vec{i}}{2c^2} & \dfrac{\left(\vec{V} - c\right)\vec{j}}{2c^2} \end{pmatrix}$$

where

$$\vec{V} = u.\vec{i} + v.\vec{j} \qquad (5)$$

$$\phi = -u.\vec{j} + v.\vec{i} \qquad (6)$$

Flow variable reconstruction process is the evaluation of Q_L and Q_R terms occurring in Eq. (3). The simplest variable reconstruction method is to take the left and right state variables Q_L and Q_R as equal to the cell center values of the corresponding sides. This reconstruction generates a first order scheme for upwinded convective terms and a second order scheme for the central discretisation of the viscous terms for one dimensional problem. Second order discretisation of the viscous terms is the most popular way in the literature, but the first order discretisation of the convective flux terms causes strong numerical diffusion errors. To reduce the diffusion error, high order variable reconstruction schemes are employed. In general, structured grid solvers use the advantage of the structure in the grid for high order reconstruction. One of the most popular reconstruction schemes used in structured grids is the Monotone Upstream-Centered Scheme for Conservation Laws (MUSCL). Although MUSCL scheme can be used on structured grids without any complexity, some ghost points (phantom nodes) are needed to be generated on unstructured grids Blazek (2015). The U-MUSCL scheme Burg (2005) which removes the necessity of these phantom nodes is used in this study.

The data reconstruction formula of U-MUSCL scheme with the variables shown in Fig. 3 is given as

$$Q_L = Q_i + \frac{k}{2}\left(Q_j - Q_i\right) + \left(1 - k\right).\nabla Q_i.\vec{r}_i \qquad (7)$$
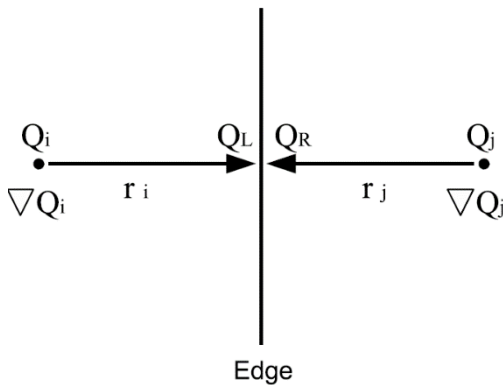

Fig. 3. Edge Variable Extrapolation.

The parameter κ, occurring in Eq. (7), is the U-MUSCL parameter and different diffusion error levels or accuracies can be obtained from different κ values. Also, it is seen from Eq. (7) that, for κ = 0, the U-MUSCL scheme reduces to piecewise linear reconstruction.

3.2 Temporal Discretisation

The general formula of implicit schemes can be obtained by linearization of the right hand side by a first order Taylor series expansion in time as it is illustrated in Eq. (8).

$$\left[\left(\frac{\vec{I}.A}{\Delta t}\right) + \left(\frac{\partial \vec{R}}{\partial \vec{Q}}\right)\right].\Delta \vec{Q}^{n+1} = -\vec{R}_i^n \qquad (8)$$

In Eq. (8), the flux Jacobian term $\left(\dfrac{\partial \vec{R}}{\partial \vec{Q}}\right)$ is a full matrix. By using the LGS method this full matrix turns into a diagonal matrix. This matrix can be written in the form as,

$$\left[\left(\frac{\vec{I}.A}{\Delta t}\right) + \left(\frac{\partial \vec{R}}{\partial \vec{Q}}\right)\right].\Delta \vec{Q} =$$

$$\begin{bmatrix} \dfrac{A}{\Delta t} + \dfrac{(R_1)_i}{(Q_1)_i} & 0 & 0 \\ 0 & \dfrac{A}{\Delta t} + \dfrac{(R_2)_i}{(Q_2)_i} & 0 \\ 0 & 0 & \dfrac{A}{\Delta t} + \dfrac{(R_3)_i}{(Q_3)_i} \end{bmatrix}\Delta\vec{Q}_i$$

$$+ \sum_{j=1}^{N_F} \begin{bmatrix} \dfrac{(R_1)_i}{(Q_1)_j} & 0 & 0 \\ 0 & \dfrac{(R_2)_i}{(Q_2)_j} & 0 \\ 0 & 0 & \dfrac{(R_3)_i}{(Q_3)_j} \end{bmatrix}\Delta\vec{Q}_j$$

(9)

where, i and j terms represents the cell itself and the neighboring cells, respectively.

The flux Jacobian term $\left(\dfrac{\partial \vec{R}}{\partial \vec{Q}}\right)$ is a 3 × 3 matrix which consists of terms representing the variation of the RHS with both the computation cell itself and the neighbouring cells. Evaluation methods and simplifications used for this term varies in different implicit schemes. In Point Gauss Seidel (PGS) method, the variation of RHS from all neighbouring cells are neglected. On the other hand, only some of these terms are neglected or approximated in a simpler way in line implicit methods. When the Line Gauss Seidel (LGS) Scheme is concerned, the cells located on the solution bands are taken as unknowns. The symbolical representation of the LGS scheme which is identical with the ACDI method is given as

$$\left[A, B, C\right]^n.\Delta\vec{Q}^n = -\vec{R}^{n+1/n} \qquad (10)$$

The $\vec{R}^{n+1/n}$ term of Eq. (10) refers to the RHS evaluated by most recent values of corresponding flow variables and [A,B,C]n corresponds to three elements of $\left[A, B, C, D, E\right]^n$ where these are each of the five elements of the flux Jacobian term. When the time integration is performed on all cells over a solution band, the $\left[A, B, C\right]^n$ terms form a tridiagonal matrix. Solution of tridiagonal type matrices are simple and time efficient when

compared with pentadiagonal or sparse matrices.

3.3 Data Management

Among a variety of data management schemes, the *Cell Based Quad Edge* approach Sedgewick and Flajolet (2013) is suitable for the implementation of ACDI as suggested by Çete (2004); Çete *et al*. (2008). In this approach, the flow variables are stored in two different arrays named as points group and cells group where a separate linked list is used to store the data about starting cells and edge values of each solution band. It then becomes possible to construct unique solution bands in an automated manner using the starting indexes stored in linked list. A sample unstructured grid portion is shown in Fig. 4. Cells are denoted by c_n and the edges of a cell by e_n . The solution bands are then given in terms of cells and the involved edges in Table 1 Çete *et al*. (2008).
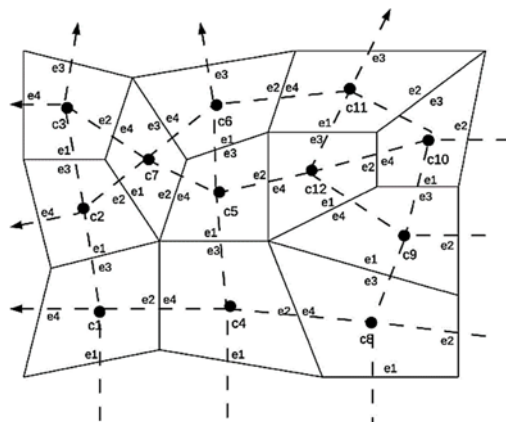
Fig. 4. A Sample Grid Portion with Cell and Edge Data.
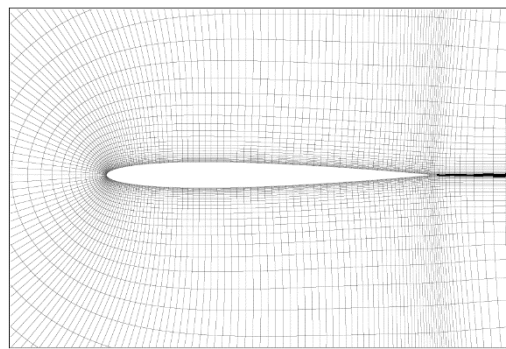
Fig. 5. 260 × 40 Structured Grid around NACA 0008 Airfoil Profile.

Table 1 Solution Bands of a Sample Unstructured Grid Portion

| e1,c1,e3→e1,c2,e3 |
|---|
| e2,c3,e3→e2,c4,e3→e4,c8,e2 |
| e1,c6,e3→e1,c7,e3→e1,c8,e3→e1,c9,e3 |
| e2,c7,e4→e2,c4,e4→e1,c5,e3 |
| e4,c2,e2→e4,c5,e2→e4,c9,e2 |
| e4,c1,e2→e4,c3,e2→e4,c6,e2 |

4.   RESULTS AND DISCUSSION

Validation of this method is done by using flow over NACA 0008 single-element airfoil for a low Reynolds number and solution of Euler equation over NACA 23012b multi-element airfoil. The advantages of ACDI and U-MUSCL schemes are shown in the first case for both structured and unstructured grids. The second case, being geometrically more complex, shows the robustness and effectiveness of the new method on flow solutions over arbitrary geometries.

Ideal convergence characteristics are satisfied with the help of sufficiently large time steps for relaxation schemes. This is also true for ACDI method and it is verified in Reference Bas¸ (2007). For all the calculations presented in this study, the CFL number is set to be 10^6 to prove the stability and efficiency of the ACDI scheme. All the present computations are done on a 3.2 GHz workstation with Intel Xeon processor with 4 GB of RAM.
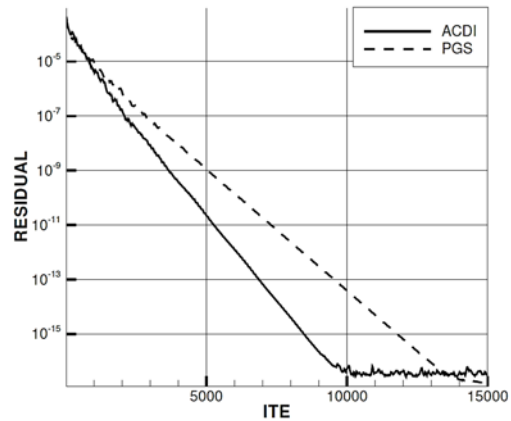
(a)
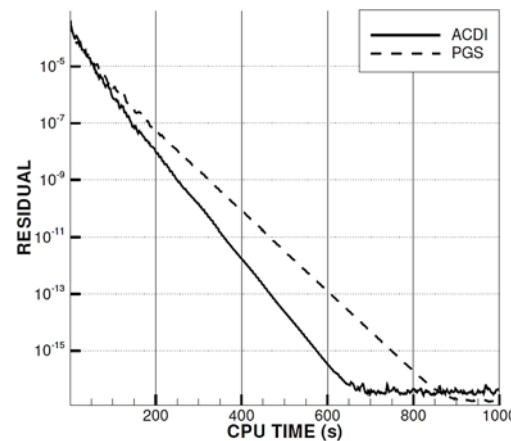
(b)

Fig. 6. Average Residual versus Number of Iteration Steps and CPU Time for 260 × 40 Structured Grid over NACA 0008 Airfoil Profile.

4.1 Laminar flow Over NACA 0008 Airfoil Profile

For the computation of laminar flow over NACA

0008, the Reynolds number is specified as 6000. And also the angle of attack of 2 is considered for the computations. Two different configurations of computational grids are used for this situation. First, a 260 × 40 C-type structured grid with 10−3 normal grid spacing on the wall is generated using a hyperbolic grid generator. The structured computational grid is shown in Fig. 5.

The residual histories for ACDI and PGS solutions are given in Fig. 6. As shown, the number of iteration steps and the convergence CPU time requirements of ACDI method are 28% and 23% more efficient, respectively, than the PGS solutions.

Fig. 8. Solution Bands of the Unstructured Grid for NACA 0008 Airfoil Calculation.

Fig. 7. Unstructured Grid Used for Naca 0008 Airfoil Calculation with 11460 Cells.

When the unstructured grid generation is concerned, DELAUNDO grid generator Delaundo (2008) is first employed for generating a triangular grid. The quadrilateral grid shown in Fig. 7 is produced by combining all these triangular cells. The grid has 11584 points and 11460 cells.

For the validation of this case, the solution bands created on the unstructured grid can be seen in the Fig. 8 and after all these solution bands are produced, there are two solutions bands for each cell pass through them twice. Also the resulting solution bands for this unstructured grid are quite different in length. The shortest band containing 14 cells and longest solution band with 1794 cells is shown on Fig. 9
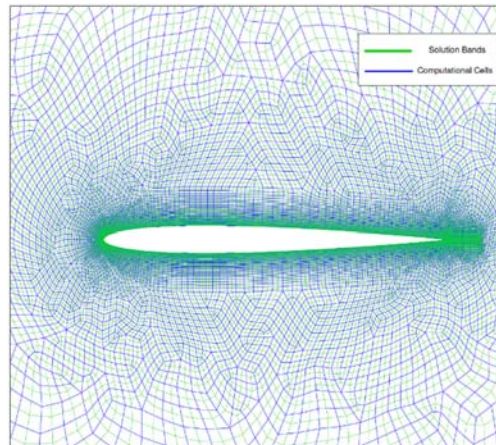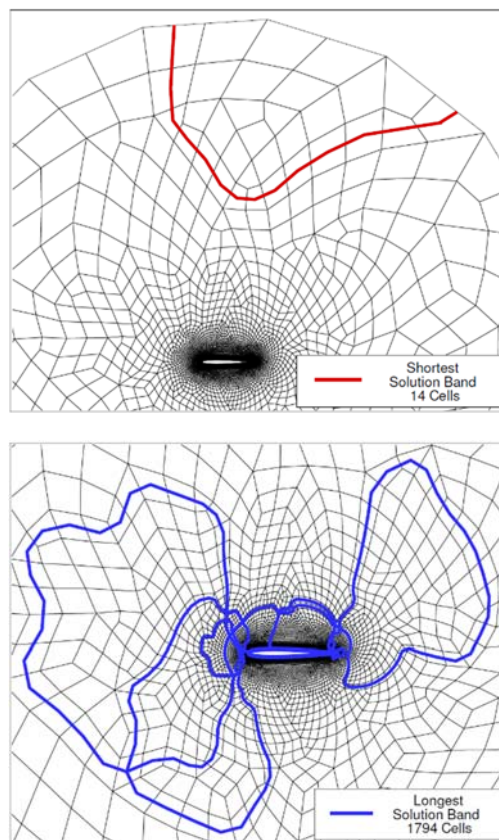

Fig. 9. The Shortest and Longest Solution Bands for the Unstructured Grid over NACA 0008 Airfoil Profile. (For each solution bands direction is not important and both of them is valid for calculation).

The solution on the unstructured grid is computed for the same flow conditions. The convergence histories are given in Fig. 10. It is seen that ACDI method is similarly 25% and 20% more efficient than the PGS method in the number of iteration steps and the total CPU time, respectively. These computational efficiencies of the ACDI method on the structured grid (23%) and on the unstructured grid (20%) are consistent with the findings of Rogers (1995) who
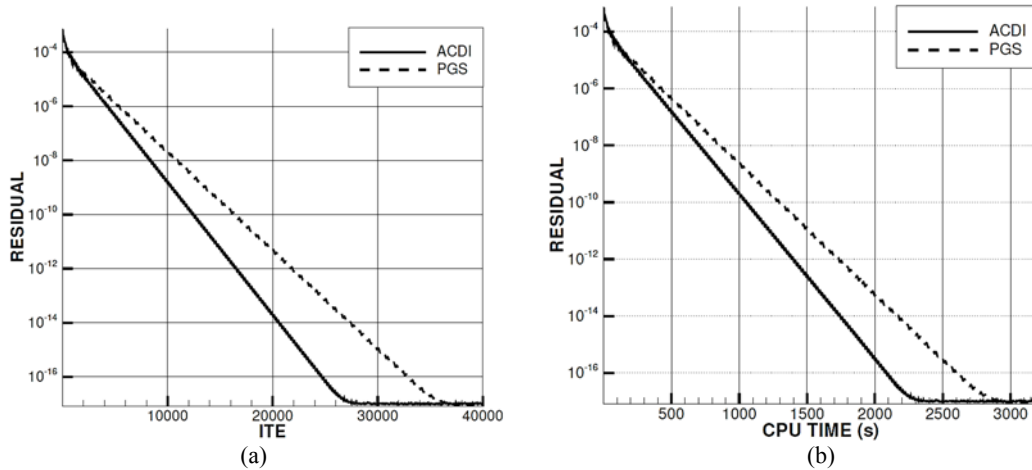
Fig. 10. Average Residual versus Number of Iteration Steps and CPU Time for the Unstructured Grid over NACA 0008 Airfoil Profile with 11460 Cells.

employs three distinct versions of structured grids over NACA 4412 airfoil and obtained efficiency gains between 14% and 30% by employing LGS scheme.

The same flow fields are computed with piecewise constant, piecewise linear and U-MUSCL ($\kappa = 0.5$) schemes on both structured and unstructured grids by using the ACDI method. The diffusive characteristics of the U-MUSCL scheme is investigated and the accuracy gains are shown graphically in Fig. 11 and Fig. 12. The solution of INS2D flow solver taken from Reference Kunz and Kroo (2000) are also used for validation. As seen, U-MUSCL scheme captures the suction peak at the leading edge more accurately and proves to be less dissipative.

4.2 Inviscid Flow Over NACA 23012b Multi Element Airfoil

The second validation case is taken as the high Reynolds number flow over the NACA 23012b multi element airfoil profile. Flow solutions over Multi element airfoils shows the effectiveness of unstructured grids.
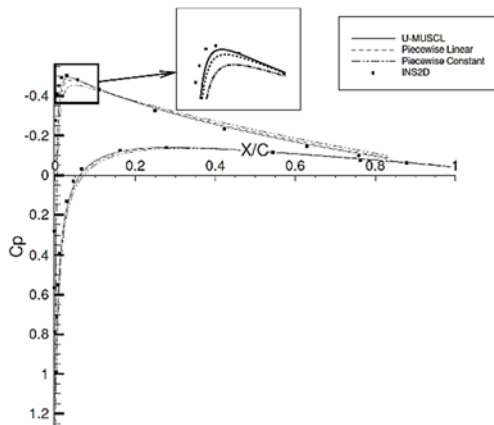

Fig. 11. Graphical Representation of the Accuracy Gain on 260×40 Structured Grid over NACA 0008 Airfoil Profile.
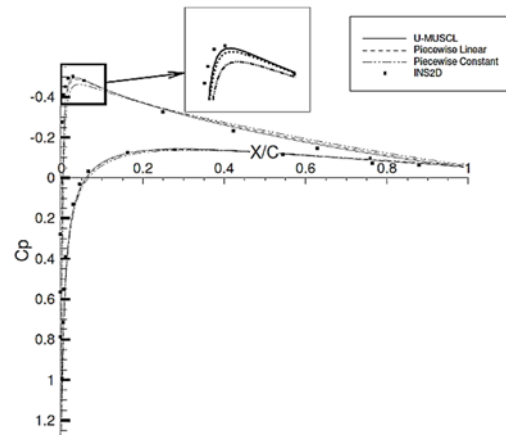

Fig. 12. Graphical Representation of the Accuracy Gain on Unstructured Grid over NACA 0008 Airfoil Profile.

The experimental data is available at a Reynolds number of 1.46×10^6 with an angle of attack of 1.0 degree for the main airfoil and 10 degrees of flap deflection Wenzinger (1938). In this study, the flow is assumed inviscid due to the lack of a turbulence model.

An unstructured grid with 12314 points and 12011 cells is employed as shown in Fig. 13.

ACDI and PGS solutions are obtained as shown in Fig. 14 for this test case. The solutions obtained by these two methods overlap as expected.

For the efficiency consideration, CFL number versus convergence iteration number graphs are plotted in the Fig. 15 for the PGS and ACDI methods for structured and unstructured grids, respectively. It can be seen clearly from the figures that ACDI method has better convergence characteristic than PGS method for the same CFL number. In other words, PGS methods require more number of iterations when compared to the ACDI method for both structured and unstructured grids.
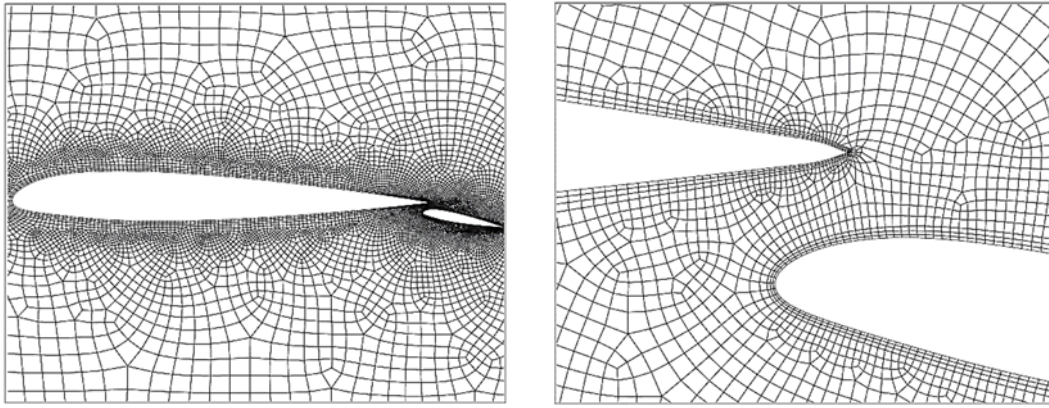
Fig. 13. Unstructured Grid Used for NACA 23012b Multi Element Airfoil Calculation with 12011 Cells.
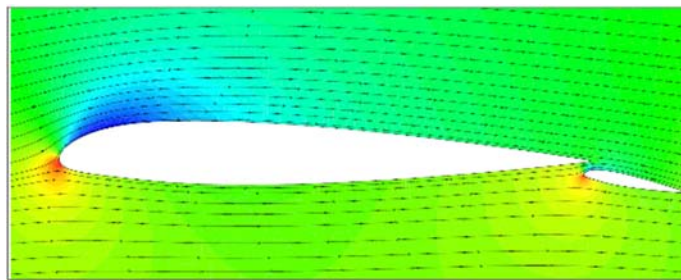

Fig. 14. The Pressure Distribution as Flood Contours over the NACA 23012b Multi Element Airfoil.
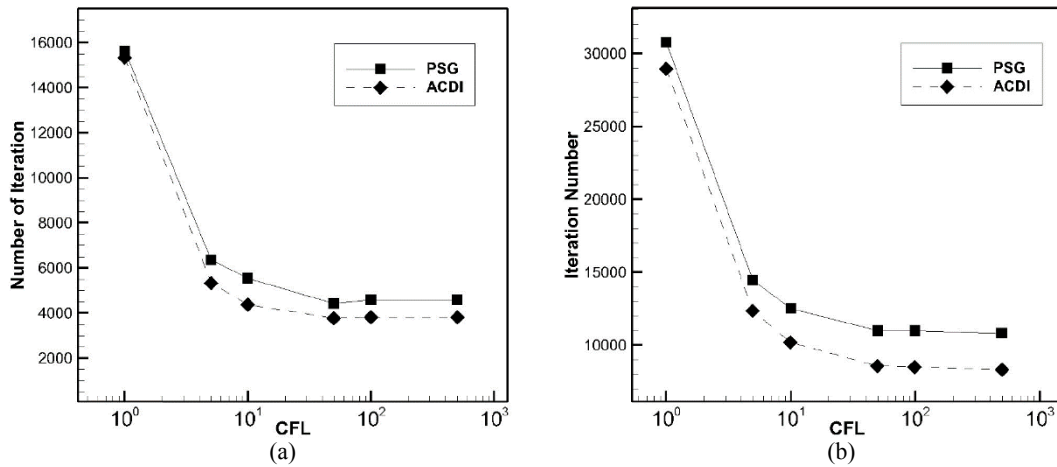

Fig. 15. Variation of Convergence Iteration Time with CFL Number on 260x40 Structured Grid and Unstructured Grid with 11584 Points.

The residual histories similarly reveal the efficiency gains of the ACDI method over the PGS method (Fig. 16): the ACDI method is 23% in iteration number and 18% in total CPU time is more efficient than the PGS method. It is seen from this test case that, ACDI method results in similar efficiency gains on different cases, independent of the geometric complexity. In Reference Rogers (1995), severe convergence problems observed on multi element airfoil validation cases.

The improved accuracy of the U-MUSCL scheme in inviscid flows is also shown in Fig. 17.

5. CONCLUSION

The primary objective of this study is to take advantage of both the computational efficiency of line implicit methods and the unstructured grids for the computation of incompressible flow over complex geometries. It is achieved by employing an Alternating Cell Directions Implicit method over unstructured quadrilateral grids. The flow fields computed compare well with experimental data and other numerical methods for validation. It is shown that the new method developed is robust, accurate,
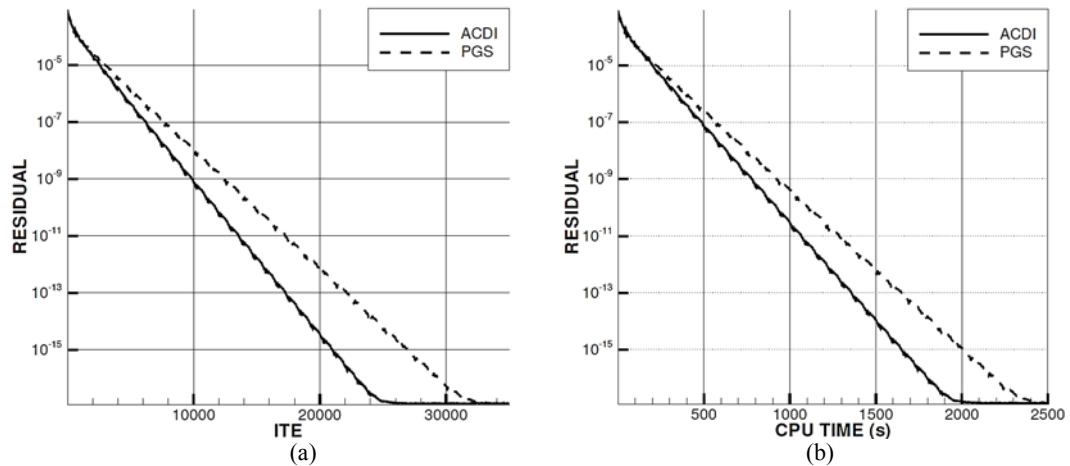
(a)   (b)

Fig. 16. Average Residual versus Number of Iteration Steps and CPU Time for Unstructured Grid over NACA 23012b Multi Element Airfoil.

efficient and flexible, and can handle complex unstructured grids with equal ease as with the structured grids. The ACDI method provides between 18% and 23% efficiency over PGS method.Based on the obtained encouraging results, extension of the ACDI method to more efficient implicit algorithms such as Approximate Factorization Pulliam and Chaussee (1981) and LU-decomposition Jameson and Turkel (1981) using ACDI as preconditioner are under way.
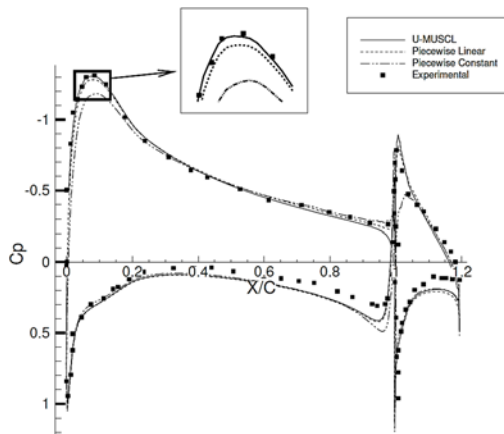

Fig. 17. Graphical Representation of the Accuracy Gain on Unstructured Grid over NACA 23012b Multi Element Airfoil.

REFERENCES

Anderson, W. K., R. D. Rausch and D. L. Bonhaus (1996). Implicit/multigrid algorithms for incompressible turbulent flows on unstructured grids. *Journal of Computational Physics* 128(2), 391–408.

Bas, O. (2007). *Development of an incompressible Navier-Stokes solver with alternating cell direction implicit method on structured and unstructured quadrilateral grids*. Ph. D. thesis, Middle East Technical University.

Blazek, J. (2015). *Computational fluid dynamics: principles and applications*. Butterworth-Heinemann.

Burg, C. O. (2005). Higher order variable extrapolation for unstructured finite volume rans flow solvers. *AIAA Paper* 4999, 2005.

Çete, A. R. (2004). *Alternating Cell Direction Implicit Method*. Ph. D. thesis, Istanbul Technical University, İstanbul, Turkey.

Çete, A. R., M. A. Yükselen and Ü. Kaynak (2008). A unifying grid approach for solving potential flows applicable to structured and unstructured grid configurations. *Computers and Fluids* 37(1), 35–50.

Çete, R. and U. Kaynak (2006). A new approximate factorization method suitable for structured and unstructured grids. *AIAA Paper* 3789.

Chan, C. and K. Anastasiou (1999). Solution of incompressible flows with or without a free surface using the finite volume method on unstructured triangular meshes. *International Journal For Numerical Methods In Fluids* 29(1), 35–57.

Chorin, A. J. (1967). A numerical method for solving incompressible viscous flow problems. *Journal of Computational Physics 2*(1), 12–26.

Delaundo (2008). Delaundo webpage. Accessed: 2008-07-27.

Duc, N. T. (1999). An implicit scheme for incompressible flow computation with artificial compressibility method. *Int. J. Numer. Fluids* 29(1), 35–57.

Jameson, A. and E. Turkel (1981). Implicit schemes and lu decompositions. *Mathematics of Computation 37*(156), 385–397.

Kaliakatsos, C., A. Pentaris, D. Koutsouris, and S. Tsangaris (1996). Application of an artificial compressibility methodology for the incompressible flow through a wavy channel. *Communications in Numerical Methods in Engineering 12*(6), 359–369.

Kunz, P. and I. Kroo (2000). *Analysis, design, and testing of airfoils for use at ultralow reynolds numbers*. In Proceedings of a Workshop on Fixed and Flapping Flight at Low Reynolds Numbers, Notre Dame. sn.

Pulliam, T. H. and D. Chaussee (1981). A diagonal form of an implicit approximate-factorization algorithm. *Journal of Computational Physics 39*(2), 347–363.

Rogers, S. E. (1995). Comparison of implicit schemes for the incompressible navier-stokes equations. *AIAA Journal 33*(11), 2066–2072.

Rogers, S. E. and D. Kwak (1990). Upwind differencing scheme for the time-accurate incompressible navier-stokes equations. *AIAA*

Journal 28(2), 253–262.

Sato, Y., T. Hino and M. Hinatsu (2003). *Unsteady flow simulation around a moving body by an unstructured navier-stokes solver.* In Proceedings of the Sixth Numerical Towing Tank Symposium, Rome, Italy.

Sedgewick, R. and P. Flajolet (2013). *An introduction to the analysis of algorithms*. Addison-Wesley.

Sheng, C. and D. L. Whitfield (1999). Multi-block approach for calculating incompressible fluid flows on unstructured grids. *AIAA journal 37*(2), 169–176.

Wenzinger, C. J. (1938). Pressure distribution over an naca 23012 airfoil with an naca 23012 external-airfoil flap.

Yuan, L. (2002). Comparison of implicit multigrid schemes for three-dimensional incompressible flows. *Journal of Computational Physics 177*(1), 134–155.